Journal of Alloys and Compounds xxx (2008) xxx–xxx

Contents lists available at ScienceDirect

Journal of Alloys and Compounds

journal homepage: www.elsevier.com/locate/jallcom

Influence of MgO addition on the synthesis and electrical properties of sintered zinc–titanate ceramics

Nina Obradovic[a,*], Miodrag Mitric[b], Maria Vesna Nikolic[c], Dragica Minic[d], Nebojsa Mitrovic[e], Momcilo M. Ristic[f]

[a] Institute of Technical Sciences of SASA, Knez-Mihailova 35/IV, 11000 Belgrade, Serbia
[b] The Vinca Institute of Nuclear Sciences, Mike Alasa 14–16, 11000 Belgrade, Serbia
[c] Institute for Multidisciplinary Research, University of Belgrade, Kneza Viseslava 1a, 11000 Belgrade, Serbia
[d] Faculty of Physical Chemistry, University of Belgrade, Studentski trg 12–16, 11000 Belgrade, Serbia
[e] Joint Laboratories for Advanced Materials of SASA, Section for Amorphous Systems, Technical Faculty Cacak, 32000 Cacak, Serbia
[f] Serbian Academy of Sciences and Arts, Knez-Mihajlova 35, 11000 Belgrade, Serbia

ARTICLE INFO

Article history:
Received 13 November 2007
Received in revised form 14 March 2008
Accepted 20 March 2008
Available online xxx

Keywords:
Ceramics
Mechanochemical processing
Sintering
X-ray diffraction

ABSTRACT

Starting mixtures of ZnO, TiO_2 and MgO (0, 1.25 and 2.5 wt.% MgO) powders were mechanically activated for 15 min in a planetary ball mill. The powders obtained were sintered non-isothermally to temperatures between 800 and 1100 °C and then held at those temperatures for 120 min. Analysis of the influence of MgO addition on the synthesis of zinc–titanate ceramics showed that its addition increased slightly the temperature at which the reaction process started, accelerated the reaction and resulted in higher sample densities. These results were correlated with the results of structural characterization using X-ray powder diffraction method and SEM analysis. Also, the results of electric resistivity, capacitance and loss tangent of the sintered samples were obtained.

1. Introduction

Spinels have awakened great interest particularly in the study of the physico-chemical properties of binary compounds and solid solutions [1]. Much attention has been paid to the synthesis and electrical properties of zinc titanate due to its attractive applications in microwave dielectrics [2,3]. Zinc titanate (Zn_2TiO_4) is an inverse spinel, which has been used as a catalyst and pigment [4].

Phase transitions in the ZnO–TiO_2 system are relatively complex, and sensitive to the starting material, additives and the preparation process [5]. The formation temperature for each of the $ZnTiO_3$, $Zn_2Ti_3O_8$ and Zn_2TiO_4 phases was shown to vary significantly with the preparation method and the Zn/Ti molar ratio of the starting materials [6–11]. A number of studies up to now have been devoted to the preparation, compound formation, crystal structure, stability, additives, as an effective way to simplify the synthesis process and improve the microwave dielectric properties, as well as the electrical properties of zinc titanates [4,12–18].

In the present work, Zn_2TiO_4 ceramics with MgO addition were prepared by a solid-state reaction. MgO has been proved to be an effective sintering aid for zinc–titanate ceramics [19]. Having in mind recent accomplishments made in the field of oxide addition to the ZnO–TiO_2 system, we presumed that MgO addition would form a solid–solution $(Zn, Mg)_2TiO_4$ and therefore stabilize the crystal structure, improve both densification and microstructures after the sintering process. The phase structure, microstructures along with electrical properties as well as dilatometer investigations of reactive sintering of zinc–titanate ceramics with MgO addition was investigated.

2. Experimental procedure

Zinc–titanate samples with addition of MgO = 0–2.50 wt.% were prepared by a conventional solid-state reaction method using ZnO (99.99% p.a. Aldrich), TiO_2 (99.99% p.a. Aldrich) and MgO (97% p.a. Merck) powders. The starting materials were mixed in ethanol with a magnetic whisk for 2 h in order to obtain homogeneity of the mixture and then dried at 120 °C for 2 h. The powders were submitted to mechanochemical treatment for 15 min in a planetary ball mill device (Fritch Pulverisette 5) at the angular speed of the supporting disc set on 400 rpm. Samples were denoted according to the added oxide, ZMTO-0, ZMTO-1.25 and ZMTO-2.50. Powders were then sieved through a 0.2 mm sieve.

X-ray diffraction patterns of powder mixtures after milling and sintering were obtained using a Philips PW 1050 diffractometer with λCu Kα radiation and a step/time scan mode of 0.05°/1 s. The morphology of obtained powders was char-

* Corresponding author. Tel.: +381 11 20 27 203; fax: +381 11 185 263.
E-mail address: ninao@bib.sanu.ac.yu (N. Obradovic).

0925-8388/$ – see front matter © 2008 Elsevier B.V. All rights reserved.
doi:10.1016/j.jallcom.2008.03.090

acterized using scanning electron microscopy (JSM-6460LV JEOL 25 kV).

In order to investigate the reactive sintering process the relative shrinkage of samples was followed by a sensitive dilatometer (B hr Ger tebau GmbH Type 702 s). Heating was carried out in air with a constant heating rate of 30 °C/min, from room temperature to 800, 900, 1000 and 1100 °C followed by holding times of 2 h. The density of specimens was calculated from precise measurements of specimen's diameter, thickness and mass.

The measurements of electrical resistivity, capacitance and loss tangent of samples were measured in the frequency range from 400 Hz to 4 MHz with a HIOKI 3532–50 LCR HiTESTER device at a constant voltage mode (amplitude 0.5 V of sinusoidal signal applied to the specimens). The "four-probe" configuration has been employed. The samples were prepared by painting silver electrodes on both sides following with thermal treatment at 120 °C for 2 h performed in order to improve the paint conductivity.

3. Results and discussion

Scanning electron images presented in Fig. 1 show a significant difference in the starting powders. MgO powder consists of regularly shaped, spherical particles with a size of 50 μ approximately (Fig. 1(a)). The surface is eroded with irregularly shaped pores with a size of 200–300 μm (Fig. 1(b)). Compared to MgO particles, ZnO and TiO_2 particles are smaller. Scanning electron images indicated polygonal sub-micron particles of ZnO powder (Fig. 1(c)) and spherical particles with a size of 150 nm of TiO_2 powder (Fig. 1(d)). Having in mind mechanical properties of MgO oxide [20], we presumed that MgO particles probably served as nuclei coated with ZnO and TiO_2 particles (Fig. 1(e))

X-ray diffraction patterns of mechanically activated starting mixtures with different amounts of MgO are presented in Fig. 2. All three analyzed mixtures were submitted to the same milling conditions, but there are significant differences. The mixture without MgO addition (ZMTO-0) has broad and low intensity ZnO diffraction peaks and very low intensing anatase (TiO_2) peaks in agreement with intensive disappearance of an ordered crystal structure after mechanical activation due to the high transfer of mechanical energy to the powder. The very first detectable traces of Zn_2TiO_4 were also present in the ZMTO-0 mixture, as expected [11].

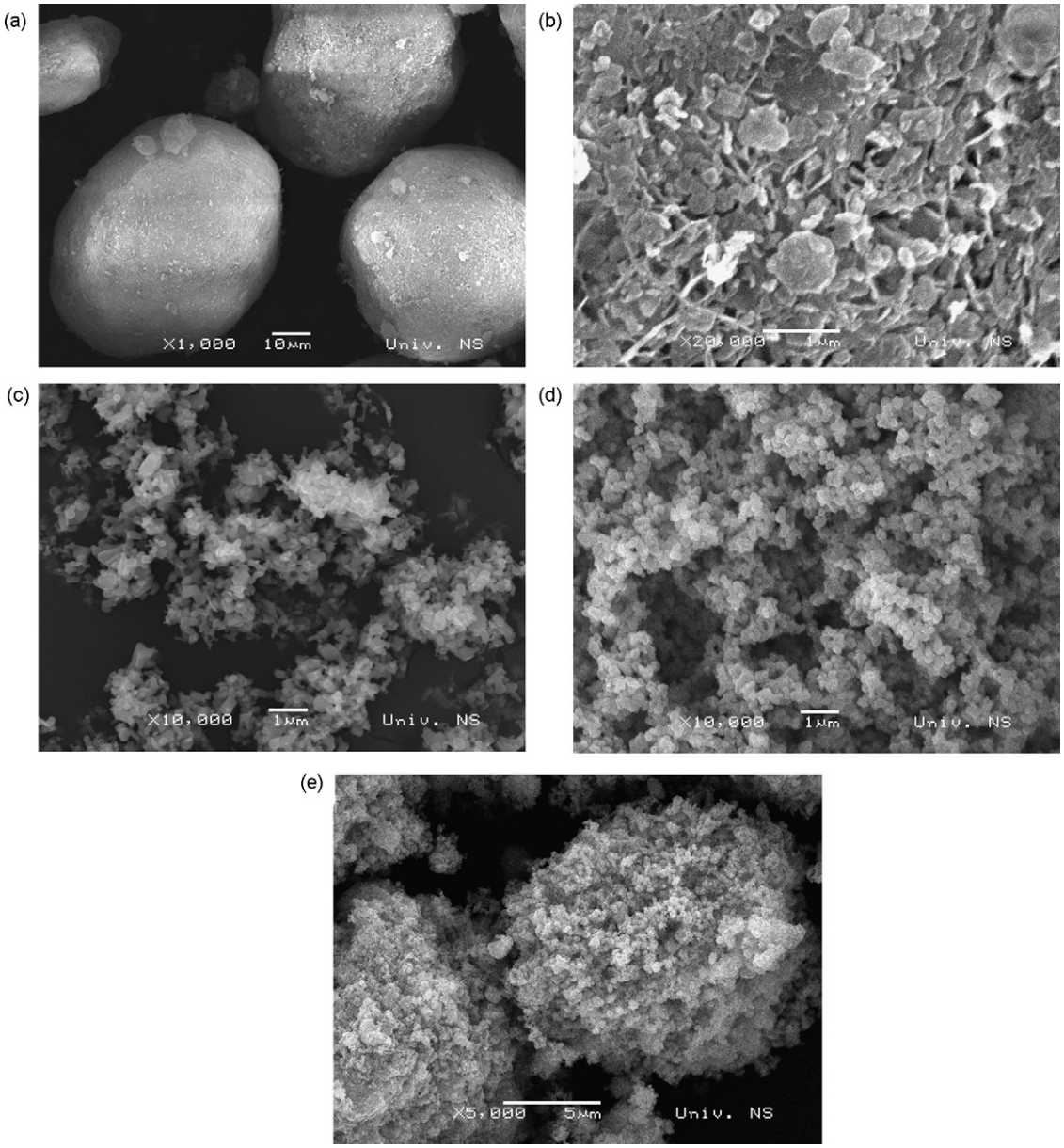

Fig. 1. Scanning electron micrographs of (a) MgO with amplification 1000, (b) MgO with amplification 20,000, (c) ZnO with amplification 10,000, (d) TiO_2 with amplification 10,000, and (e) ZMTO-1.25 with amplification 5000.

Please cite this article in press as: N. Obradovic, et al., J. Alloys Compd. (2008), doi:10.1016/j.jallcom.2008.03.090

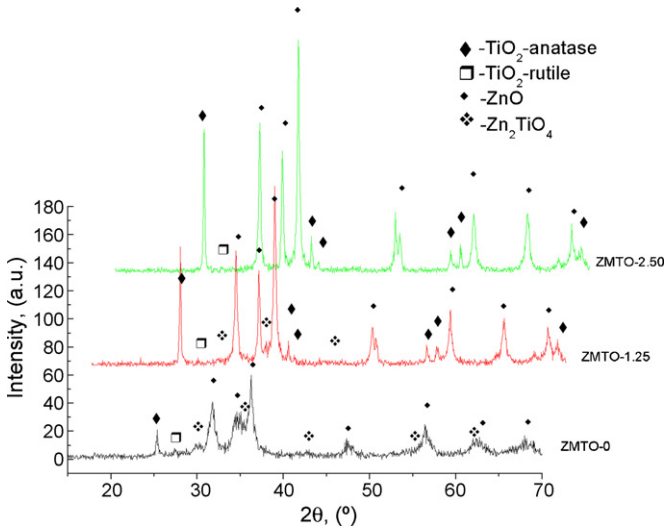

Fig. 2. X-ray diffraction patterns of mechanically activated starting mixtures with different amounts of MgO.

In powders with MgO (ZMTO-1.25 and ZMTO-2.50) all peak intensities are sharper, showing that the presence of rigid and stable MgO particles obstructs both mechanical treatment and mechanochemical reactions (Young modulus for MgO, ZnO and TiO_2 are 45, 108 and 116, respectively [20]). Barely visible traces of the zinc titanate phase are also detectable in ZMTO-1.25 but not in the ZMTO-2.50 mixture. MgO peaks were not detected.

Table 1
Densities of samples before (ρ_0) and after (ρ_s) the sintering process given in % TD

Sample	ρ_0/ρ_s (800 °C)	ρ_0/ρ_s (900 °C)	ρ_0/ρ_s (1000 °C)	ρ_0/ρ_s (1100 °C)
ZMTO-0	67.51/70.08	67.51/70.97	67.53/80.00	67.53/90.63
ZMTO-1.25	64.33/68.84	64.15/70.65	64.25/77.60	64.21/90.55
ZMTO-2.50	62.51/65.61	62.61/67.16	62.47/78.88	62.59/89.58

Fig. 3(a) shows the relative shrinkage of samples as a function of time during heating and 2 h holding at 800, 900, 1000 and 1100 °C for ZMTO-0 samples, obtained by dilatometer. Fig. 3(b)–(d) shows relative shrinkage along with the derivative curves of ZMTO-0, ZMTO-1.25 and ZMTO-2.50 sintered at 1100 °C for 2 h, respectively. Thus, one can notice that intensive sintering of mixtures sintered at 1000 and 1100 °C is accompanied by characteristic shrinkage and an expansion just before the sintering process, which is the characteristic of spinel formation at lower temperatures [17]. Contrary to that, the solid-state reaction in the samples sintered at 800 and 900 °C, preceded in a quite different manner. First, the characteristic maximum of zinc titanate formation is not observed, and secondly the sintering process is far away from the final stage.

Shrinkage curves of ZMTO-1.25 and ZMTO-2.50 mixtures exhibited the same trend as ZMTO-0. Analyses of curves presented in Fig. 3(b)–(d) indicate that MgO addition shifts the onset of the reaction process to higher temperatures. As the inclination of dilatometric curve is defined by reaction rate, one can notice that larger inclination indicate the faster reaction within these powders. Hence, we assume that the MgO addition accelerates the spinel formation. This is correlated to the fact that the thermodynamic stability of system was actually improved due to magnesium substitution [21,22]. We concluded, also, that MgO

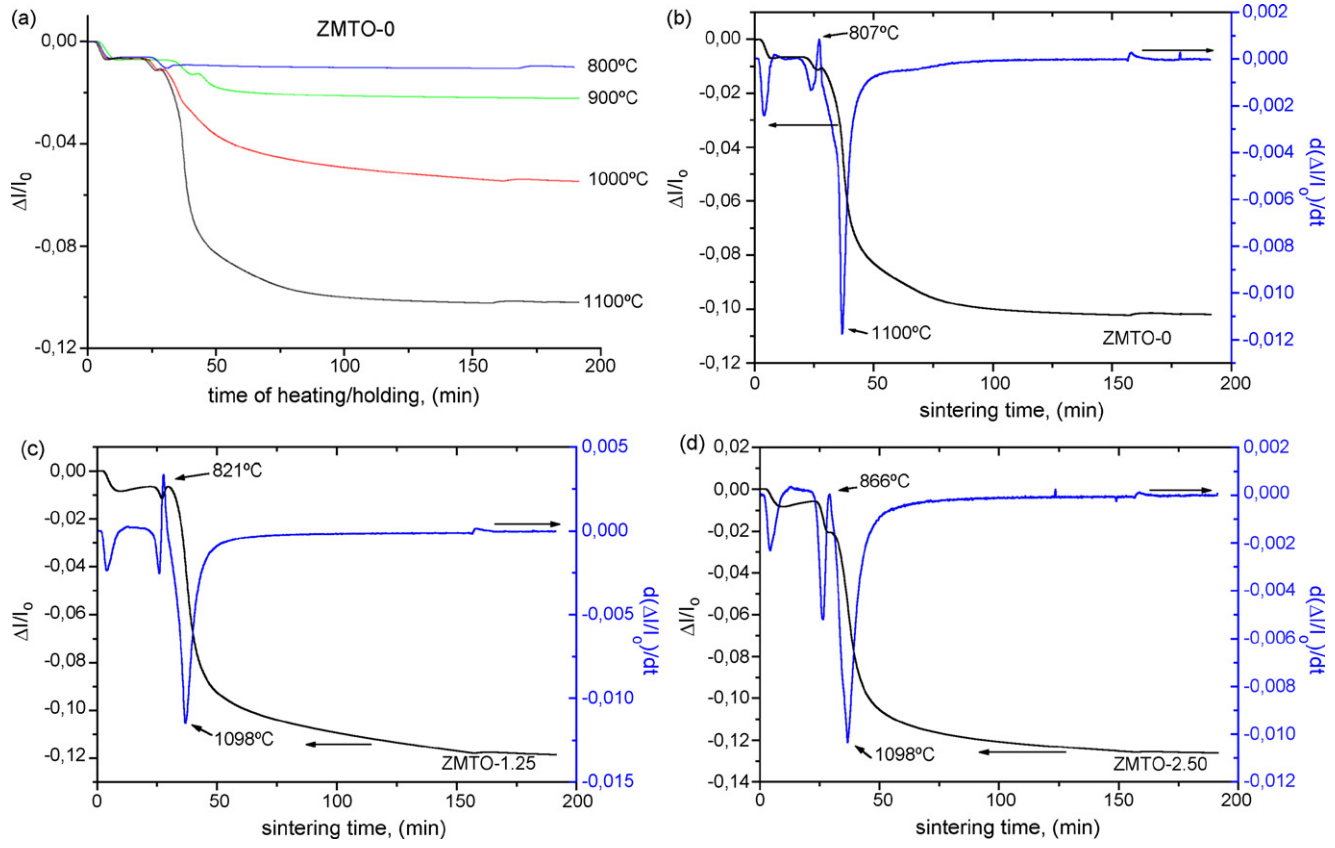

Fig. 3. (a) Relative shrinkage of ZMTO-0 as a function of time during heating to 800, 900, 1000 and 1100 °C and 2 h holding. Relative shrinkage and derivative curve for (b) ZMTO-0 sintered for 2 h at 1100 °C, (c) ZMTO-1.25 sintered for 2 h at 1100 °C, and (d) ZMTO-2.50 sintered for 2 h at 1100 °C.

Please cite this article in press as: N. Obradovic, et al., J. Alloys Compd. (2008), doi:10.1016/j.jallcom.2008.03.090

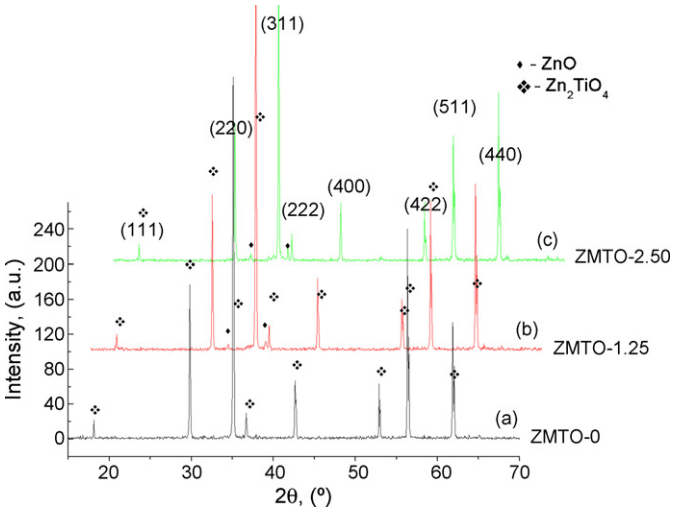

Fig. 4. X-ray diffraction patterns of (a) ZMTO-0, (b) ZMTO-1.25 and (c) ZMTO-2.50 sintered at 1100 °C for 2 h.

addition has no effect on sintering temperatures. The greatest shrinkage was obtained for samples with 2.50 wt.% MgO sintered at 1100 °C as shown in Table 1, given in percentages of theoretical densities (TD_{ZMTO-0} = 5.060 g/cm^3, $TD_{ZMTO-1.25}$ = 5.035 g/cm^3 and $TD_{ZMTO-2.50}$ = 5.010 g/cm^3), as expected [13].

Fig. 4 shows the X-ray diffraction patterns of (a) ZMTO-0, (b) ZMTO-1.25 and (c) ZMTO-2.50 sintered at 1100 °C for 2 h. It is clearly visible that after heating we have a pure zinc titanate phase in sample without MgO and zinc titanate phase with a small amount of ZnO in samples with MgO addition. All samples sintered at 800 °C (Fig. 5(a)–(c)) for 2 h contained small amounts of ZnO and with increasing sintering temperature the ZnO concentration decreased but was still detectable in samples sintered at 1100 °C with MgO addition. Also, the reflections are sharp and intensive due to recrystallization.

Recovery of the activated material, the disappearance of defects and grain growth are processes that occur during sintering. No MgO phase was detected for all the samples examined. It is important to note that the peaks of the sintered samples shifted towards higher angles with an increase in MgO content. The *a*-axis of the $(Zn, Mg)_2TiO_4$ linearly decreased as the amount of MgO increased (*a* = 8.4760, 8.4709 and 8.4649 A for ZMTO-0, ZMTO-1.25 and ZMTO-2.50, respectively), obeying the generally known Vegard's law. The decreased *a*-axis lattice parameters could be explained by the difference in the ionic crystal radii of Zn^{2+} and Mg^{2+} which are 0.74 and 0.66 A, respectively, tending to make it easy to substitute the zinc site by a magnesium ion [21]. Consequently, one can conclude that the substituted Mg stabilizes the crystalline structure. That statement is clearly visible while observing the decrease in *a*-axis parameter and its approaching to the value 8.4150 A observed from zinc titanate JCPDS pattern no. 86–0156.

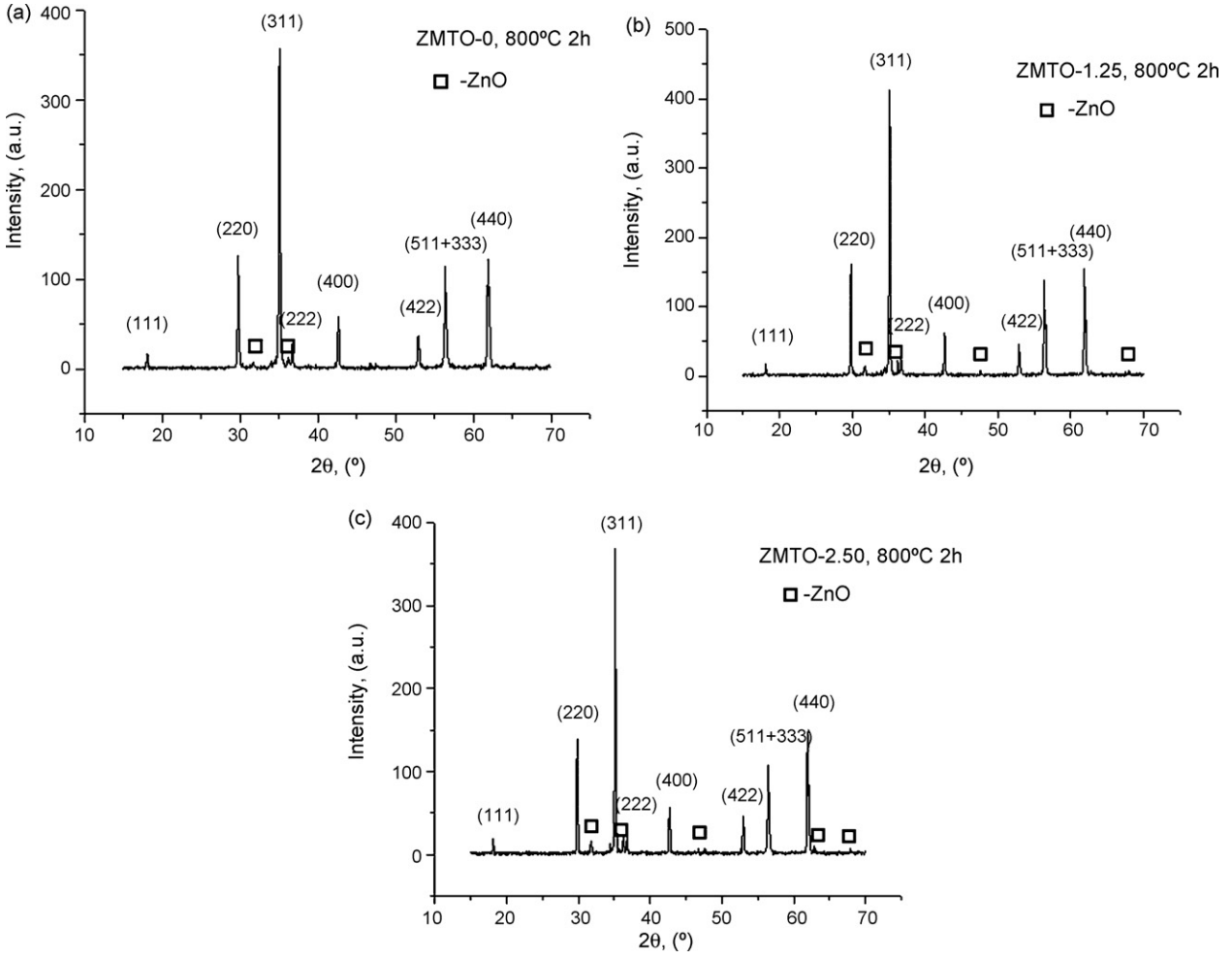

Fig. 5. X-ray diffraction patterns of (a) ZMTO-0, (b) ZMTO-1.25, and (c) ZMTO-2.50 sintered at 800 °C for 2 h.

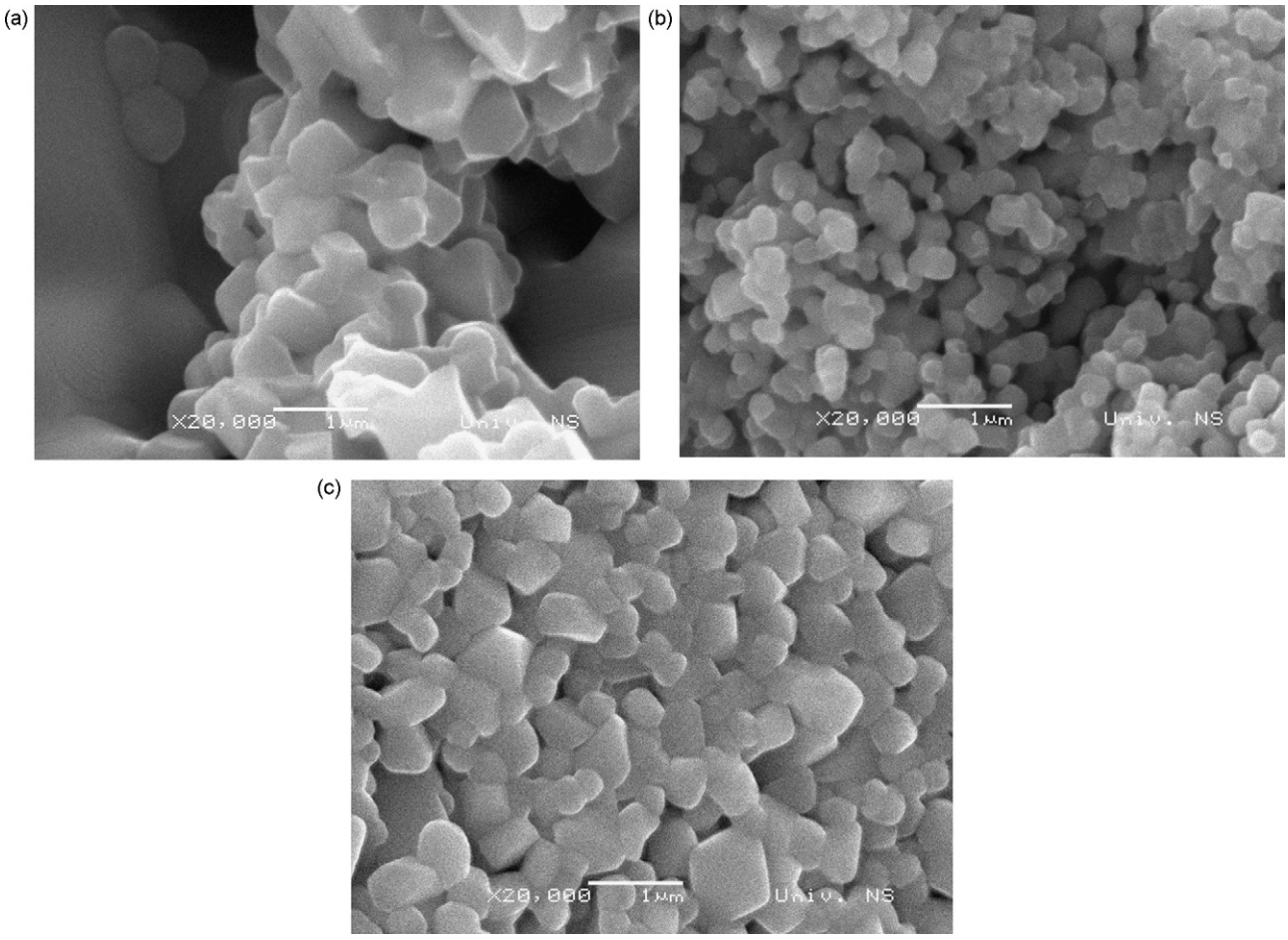

Fig. 6. Scanning electron micrographs of (a) ZMTO-0, (b) ZMTO-1.25, and (c) ZMTO-2.50 powders sintered at 1100 °C for 2 h.

Scanning electron images presented in Fig. 6 show a significant difference in powders sintered at 1100 °C with different amount of MgO. Evolution of microstructural constituents, grains and pores occurs during the sintering process, where along with increasing of both the temperature and sintering time, adequate processes of grain growth and decreasing pore size take place. The micrograph of ZMTO-0 indicates the presence of well-formed zinc–titanate polygonal grains approximately 700 nm in diameter. Microstructures of ZMTO-1.25 and ZMTO-2.50 show some similarities probably due to formation of a solid–solution [9] and more homogeneous grain distribution compared to ZMTO-0. Observing the microstructure of ZMTO-1.25 (Fig. 6(b)), we can conclude that the grains are smaller and spherical, approximately 200 nm in size with a more uniform pore distribution. More pronounced densifications along with grains that are approximately 300–400 nm in size are noticeable for ZMTO-2.50 (Fig. 6(c)). According to our analysis the most homogenous microstructure was obtained for the sample with 2.50 wt.% MgO sintered at 1100 °C.

The results of microstructure development are in accordance with dielectric properties of the samples. The values of density changes during the sintering process (d_s, given in %), quality factor (Q), relative dielectric permittivity (ε_r) and specific resistance (ρ, given in Ω m) of samples sintered at 1100 °C for 2 h are given in Table 2.

Table 2
Relative shrinkage and electrical properties (at the 4 MHz frequency) of samples ZMTO-0, ZMTO-1.25 and ZMTO-2.50 sintered at 1100 °C for 2 h

Sample	d_s (%)	ε_r	Q	tg δ ($\times 10^{-3}$)	ρ (Ω m)
ZMTO-0	25.50	7.16	131	7.63	1.76
ZMTO-1.25	29.70	13.72	83.5	11.97	3.92
ZMTO-2.50	30.12	13.82	130	7.69	2.87

The electrical measurements pointed out that relative dielectric permittivity of the specimens increased with MgO addition and is in a good agreement with literature data. It is believed that the density play an important role in controlling dielectric loss, as has been often found in other microwave dielectric materials [10]. The Q value is generally affected not only by the lattice vibrational modes, but also by the pores, the second phases, the impurities, the lattice defects, crystallizability and inner stress [23]. According to our analysis, since a higher density or a greater shrinkage during sintering resulted in a higher dielectric permittivity owing to the lower porosity for the fixed sintering temperature and since the amount of the secondary phase is very small, as observed from XRPD, the effect of the poly-phase mixture on dielectric permittivity change is less sensitive than the density effect [24]. In addition, Zn_2TiO_4 doped with different amounts of Mg enhances the specific electrical resistivity. The influence of the Mg impurities is that the Mg atoms in Zn_2TiO_4 act as scattering centers [13,14].

4. Conclusions

The phase composition in ZnO–TiO_2 solid solutions with the addition of MgO = 0–2.50 wt.% along with the microstructures, electrical properties and the analyses of non-isothermal sintering was studied. The main conclusions are:

Please cite this article in press as: N. Obradovic, et al., J. Alloys Compd. (2008), doi:10.1016/j.jallcom.2008.03.090

- MgO is a very rigid and stable oxide compared to ZnO and TiO_2 that are brittle and soft with spherical particles with a size of 50 μ approximately. It probably serves as nuclei coated with ZnO and TiO_2 particles, which are much smaller, and therefore its addition obstructs both mechanical activation and the beginning of the mechanochemical reaction.
- The reaction temperatures are shifted to higher temperatures and the reaction of spinel formation is accelerated with MgO addition. The thermodynamic stability of system was actually improved due to the magnesium substitution. Also, densities of all three mixtures increase with sintering temperatures reaching their maximum for mixtures with MgO addition at 1100 °C, as expected.
- The sintered samples crystallized in a solid solution along with a small amount of ZnO in doped samples. The lattice parameter of the samples decreased with MgO content, which indicates that MgO addition stabilizes the crystal structure of zinc titanate.
- For the activation and sintering conditions we used, a higher density and homogeneity of morphology are dominantly responsible for the higher values of relative dielectric permittivity. Also, MgO addition increased the relative dielectric permittivity as well as specific resistance, as expected.

References

[1] Y.-M. Chiang, D.P. Birnie III, W.D. Kingery, Physical Ceramics—Principles for Ceramic Science and Engineering, Wiley, New York, 1997.
[2] H.T. Kim, J.D. Byun, Y.H. Kim, Mater. Res. Bull. 33 (1998) 963–973.
[3] H.T. Kim, J.D. Byun, Y.H. Kim, Mater. Res. Bull. 33 (1998) 975–986.
[4] A.C. Chavez, S.J.G. Lima, R.C.M.U. Araujo, M.A.M.A. Maurera, E. Longo, P.S. Pizani, L.G.P. Simoes, L.E.B. Soledade, A.G. Souza, I.M.G. Dos Santos, J. Solid State Chem. 179 (2006) 985–992.
[5] X.C. Liu, F. Gao, L.L. Zhao, C.S. Tian, J. Alloys Compd. 436 (2007) 285–289.
[6] C.-L. Huang, M.-H. Weng, C.-C. Yu, Ceram. Int. 27 (2001) 343–350.
[7] C.-L. Huang, M.-H. Weng, C.-T. Lion, C.-C. Wu, Mater. Res. Bull. 35 (2000) 2445–2456.
[8] Y. Zheng, V. Zhao, W. Lei, S. Wang, Mater. Lett. 60 (2006) 459–463.
[9] C.-L. Huang, C.-S. Hsu, R.-J. Lin, Mater. Res. Bull. 36 (2001) 1985–1993.
[10] J. Zhu, E.R. Kipkoech, W. Lu, J. Eur. Soc. 26 (2006) 2027–2030.
[11] N. Obradovic, N. Labus, T. Sreckovic, D. Minic, M.M. Ristic, Sci. Sint. 37 (2005) 123–129.
[12] Y.R. Wang, S.F. Wang, Y.M. Lin, Ceram. Int. 31 (2005) 905–909.
[13] Y.S. Chang, Y.H. Chang, I.G. Chen, G.J. Chen, Solid State Commun. 128 (2003) 203–208.
[14] Y.S. Chang, Y.H. Chang, I.G. Chen, G.J. Chen, Y.L. Chai, S. Wu, T.H. Fang, J. Alloys Compd. 354 (2003) 303–309.
[15] X. Liu, et al., Mater. Res. Bull. (2007), doi:10.1016/j.materresbull.2007.03.029.
[16] S.K. Manik, P. Bose, S.K. Pradhan, Mater. Chem. Phys. 82 (2003) 837–847.
[17] N. Obradovic, N. Labus, T. Sreckovic, M.M. Ristic, Mater. Sci. Forum 494 (2005) 411–416.
[18] R.L. Millard, R.C. Peterson, B.K. Hunter, Am. Miner. 80 (1995) 885–896.
[19] M.P. Seabra, A.N. Salak, V.M. Ferreira, J.L. Ribeiro, L.G. Vieira, J. Eur. Ceram. Soc. 24 (2004) 2995–3002.
[20] M. Winter, http://www.webelements.com, as on July 01 2007.
[21] H.T. Kim, S. Nahm, J.D. Byun, J. Am. Ceram. Soc. 82 (1999) 3476–3480.
[22] N. Obradovic, S. Stevanovic, M. Mitric, M.V. Nikolic, M.M. Ristic, Sci. Sint. 39 (2007) 241–248.
[23] W. Lei, Mater. Lett. (2007), doi:10.1016/j.matlet.2007.01.017.
[24] N. Obradovic, et al., Ceram. Int. (2007), doi:10.1016/j.ceramint.2007.09.020.

Please cite this article in press as: N. Obradovic, et al., J. Alloys Compd. (2008), doi:10.1016/j.jallcom.2008.03.090